Cation displacements and the structures of the superconducting pyrochlore osmates AOs_2O_6 (A=K, Rb, and Cs)

Rosa Galati,[1] Charles Simon,[1] Paul F. Henry,[2] and Mark T. Weller[1]
[1]*School of Chemistry, University of Southampton, Southampton SO17 1BJ, United Kingdom*
[2]*Institut Laue Langevin, 6 rue Jules Horowitz, Boite Postale 156X, 38042 Grenoble Cedex 9, France*
(Received 8 January 2008; revised manuscript received 29 February 2008; published 21 March 2008)

Variable temperature, 2 K$<T<$500 K, powder neutron diffraction studies of the beta-pyrochlores AOs_2O_6 and $ANbTeO_6$, A=K, Rb, and Cs, have been undertaken. Anomalous behaviors in the lattice parameter variations as a function of temperature for the superconducting osmates with A=K, and to a lesser extent for A=Rb, are associated with local, static displacements of the alkali metal cation, which occur below ~80 K. These displacements are random around the 8*b* position as modeled in the space group *Fd*-3*m*; no evidence for decrease in symmetry from *Fd*-3*m* was observed for any sample above 2 K. For the nonsuperconducting $ANbTeO_6$, A=K, Rb, and Cs, phases, similar structural and lattice parameter behaviors are observed with localization of the potassium ions in $KNbTeO_6$ below ~30 K.

DOI: 10.1103/PhysRevB.77.104523 PACS number(s): 61.05.fm, 61.50.Ks, 61.66.Fn, 65.40.De

I. INTRODUCTION

Members of the family of superconductors, AOs_2O_6 (A=Cs, Rb, and K), adopting the β-pyrochlore structure, have reported T_c of 3.6, 6.3, and 9.6 K, respectively.[1–3] This structure is normally described in the space group *Fd*-3*m* with *A*, *B*, and O occupying the 8*b*, 16*c*, and 48*f* sites, respectively. Recent structural work on these β-pyrochlores has concentrated on KOs_2O_6, with two groups proposing different crystal structures from single crystal x-ray data. Schuck *et al.*[4,5] have stated that between 100 and 400 K, weak additional reflections are observed, which violate *Fd*-3*m* symmetry and suggest a symmetry reduction to *F*-43*m*. This is in contrast to Yamaura *et al.*[6] who found no extra reflection in their data collected between 5 and 300 K and concluded that the structure is best described in *Fd*-3*m*. Both groups have demonstrated that the modeled atomic displacement parameter (ADP) of the potassium ion at room temperature is unusually large when compared to those of other ions. These observations agree with the band structure calculations of Kuneš *et al.* where an instability in the optic mode of the K^+ ion was found to result in the "rattling" behavior.[7] Very recent work by Hiroi and co-workers[8–10] on KOs_2O_6 has provided evidence for a possible phase transition, of first order, at T_p=7.5 K in the superconducting state in zero magnetic field. This transition was believed to be associated with the rattling of K^+ located in an anharmonic potential created by the Os-O units and may have a structural origin, but neither symmetry change nor cell doubling was detected in that work. Hydration of KOs_2O_6 to form $KOs_2O_6 \cdot 0.1H_2O$ causes displacement of some of the potassium ions thus allowing water molecule to enter the structure; this degrades the superconducting properties.[11]

The previous studies of thermal dependence of the structures of AB_2O_6 phases have all been undertaken using single crystal x-ray diffraction with the limitations inherent in that method. These include the relative insensitivity to light atom positions and difficulties in determining accurate and precise lattice parameters; furthermore, very low temperature studies, below 20 K, are problematic with x rays due to absorption by the cryogenic equipment. In order to answer the various issues associated with the structures of these materials as a function of temperature, we have undertaken a detailed powder neutron diffraction study of each of the materials KOs_2O_6, $RbOs_2O_6$, and $CsOs_2O_6$ between 1.5 and 500 K (350 K, A=Cs). In order to determine whether the behaviors observed are specific to the superconducting beta osmate pyrochlores, we have also studied a second family of beta-pyrochlores $ANbTeO_6$, A=K, Rb, and Cs, in an identical fashion.

II. EXPERIMENT

Polycrystalline KOs_2O_6 was prepared by reaction of appropriate quantities of high-purity OsO_2 (0.862 g, Alfa aesar, 99.99%) and KO_2 (0.138 g, Aldrich). These materials were ground together thoroughly in a dry box, pressed into a pellet, and placed into silica ampoule together with a small gold tube containing 0.13 g of Ag_2O to create an oxidizing atmosphere. The ampoule was sealed under vacuum and heated to 723 K at a rate of 100 K h^{-1} and maintained at this temperature for 16 h before furnace cooling. Bulk KOs_2O_6 can be reliably synthesized using this method but is not single phase and contains small amounts of OsO_2 (~5%), $KOsO_4$ (~20%), and OsO_4 (visibly observed as coating the wall of the tube and some crystallites). OsO_4 rapidly evaporates from the product at room temperature in a stream of air (caution OsO_4 is very toxic by inhalation, ingestion, or skin contact). $RbOs_2O_6$ was prepared by reaction of RbO_2 (0.41 g, synthesized from Rb metal and O_2 in liquid ammonia) and OsO_2 (1.59 g, Alfa aesar, 99.99%) at an elevated oxygen pressure (0.13 g Ag_2O); the silica tube was heated at 100 K h^{-1} to 873 K and maintained at this temperature for 14 h before furnace cooling. $CsOs_2O_6$ was prepared by reaction of CsO_2 (0.135 g, synthesized from Cs metal and O_2 in liquid ammonia) and OsO_2 (0.365 g, Alfa aesar, 99.99%) in the presence of 0.13 g of Ag_2O. The silica tube was heated at 100 K h^{-1} to 943 K and maintained at this temperature for 14 h before furnace cooling.

All $AOsO_4$ phases, A=K, Rb, and Cs, can be removed from the mixed-phase products by washing with water or other polar solvents though exposure to water, air, or wet solvents, which results in the rapid, reversible, uptake of water into the KOs_2O_6 pyrochlore structure channels.[11] For A=Rb and Cs, no such uptake of water occurs. In order to produce a near pure polycrystalline sample of each of AOs_2O_6 phase, the products from the sealed tube reactions were washed with water for 30 min and then dried in a nitrogen atmosphere at 600 K for 12 h; the products from such washing-drying protocols have been shown to be structurally identical to pyrochlore materials handled only in dry conditions.[11] Following this procedure, all handling was undertaken in strictly dry (<2 ppm H_2O) atmospheres. X-ray diffraction patterns for all samples were collected at 298 K using a Siemens D5000 diffractometer, operating with a primary monochromator λ=1.54056 Å, over a 2θ range of 10°–110° with a step size of 0.02° over 15 h under dried nitrogen. Profiles indicated that for all the washed and dried samples, the main observed peaks could be indexed using a cubic cell with $a \sim 10$ Å with the space group Fd-3m; a few very weak peaks $I/I_0 < 0.04$ could be assigned to OsO_2. The 2–3 g samples of each osmate pyrochlore, A=K, Rb, and Cs, were obtained by combining the products from several syntheses under identical conditions and used for powder neutron diffraction studies.

Samples of $ANbTeO_6$ (A=K, Rb, and Cs) were prepared from stoichiometric quantities of ANO_3 (all Aldrich, 99.9%), Nb_2O_5 (Aldrich, 99.9%), and $Te(OH)_6$ (Aldrich). The starting materials were initially ground together and annealed as a powder for 24 h at 723 K to allow the volatile components disassociate. The sample was then allowed to cool, reground, and pelletized before being calcined for a further 24 h at 973 K. Large, phase pure from powder x-ray diffraction, samples (~5 g) were readily produced in this manner.

Neutron diffraction data were recorded on the high flux D20 diffractometer at the Institut Laue-Langevin, Grenoble in the 1.5–500 K temperature range using a cryofurnace. The sample was loosely sealed inside a vanadium can with a small header space; instrument calibration runs were immediately carried out prior to and after the experiments. For all osmates, data were initially collected in the 2θ=10°–150° range with a wavelength λ=1.87 Å; typically, a longer period, 20 min, data set was initially collected at 1.5 K with shorter data collections at 4 and 7 K. Thereafter, a continuous ramp rate of between 1 and 2 K min^{-1} was used between 10 and 500 K (A=K and Rb) or 350 K (A=Cs) with data collections in 1 min blocks. For KOs_2O_6, a second set of data was collected between 2 and 12 K with a 0.2 K min^{-1} ramp rate; for $RbOs_2O_6$, data were analyzed in combination with additional neutron diffraction profiles previously collected.[12] The $ANbTeO_6$ (A=Cs, Rb, and K) phases were studied using a similar temperature and data collection regimes.

III. DATA ANALYSIS

A. AOs_2O_6, A=K, Rb, and Cs

Initial data analysis for all three materials was undertaken in the Fd-3m space group using the standard beta-pyrochlore

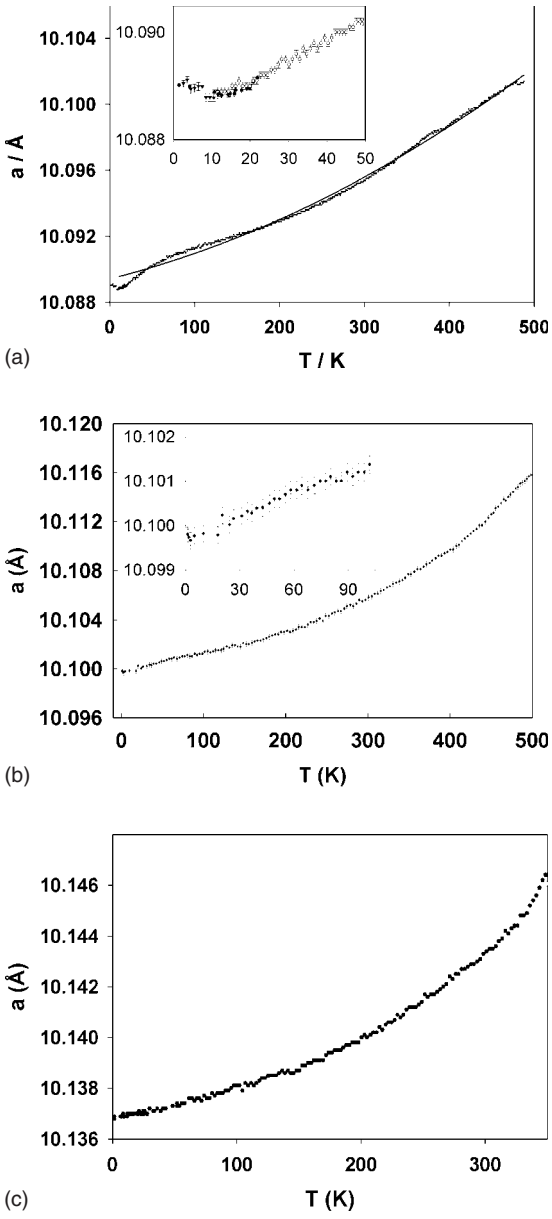

FIG. 1. (a) Variation of the lattice parameter as a function of temperature for KOs_2O_6; the inset expanded low temperature regime. Data collections in 10–500 K run (○), longer period, low temperature, below 10 K, data collections (●), and second data collection 2–12 K (▼). The curve fitted to 10–500 K data represents the best fit using a Grüneisen-type behavior. (b) Variation of the lattice parameter as a function of temperature for $RbOs_2O_6$. The inset expanded low temperature regime. (c) Variation of the lattice parameter as a function of temperature for $CsOs_2O_6$.

description by means of the GSAS/EXPGUI suite programs.[13,14] In general, this gave a good fit to the data and allowed extraction of the structural model independent parameters such as the lattice parameter. Figures 1(a)–1(c) plot the lattice parameters as a function of temperature for the three materials AOs_2O_6, A=K, Rb, and Cs; Absolute values were in accordance with previous studies and the general variation as a function of temperature typical of thermal expansion. However, the thermal expansions of the cells are small, *vide infra*,

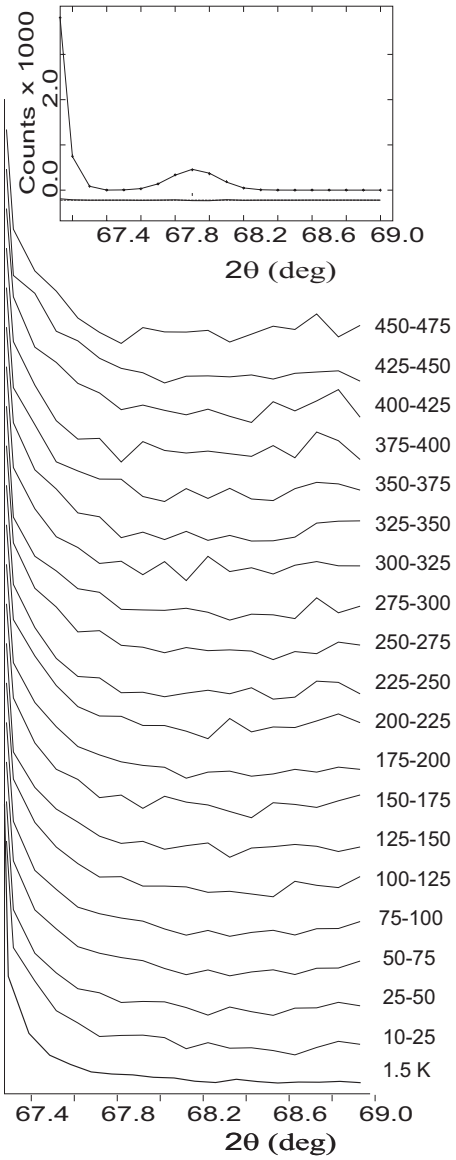

FIG. 2. Powder neutron diffraction data from KOs_2O_6 in the angular range of 67.1°–69° corresponding to the expected position of the 600 reflection in $F4\text{-}3m$. The inset shows the calculated powder pattern in this region based on the model of Schuck *et al.* (Ref. 5).

and do not perfectly occur in accordance with simple Grüneisen theory particularly for $A=\mathrm{K}$. For $A=\mathrm{Rb}$, we have previously noted a slight plateau of the lattice parameter as a function of temperature between 60 and 100 K after an initial steeper increase to 60 K, and this effect is again observed here [Fig. 1(b)]. In each case, the thermal expansion is relatively small for oxides as reflected in the low average thermal expansion parameters for these materials between 10 and 350 K with $\alpha=2.19\times10^{-6}$ K^{-1} (K) and 2.28×10^{-6} K^{-1} (Rb), in excellent agreement with the value previously reported using other neutron diffraction data of $\alpha=2.0\times10^{-6}$ K^{-1} (Rb) and 2.69×10^{-6} K^{-1} (Cs) (cf. typical α for a perovskite oxide of 10×10^{-6} and 8.1×10^{-6} K^{-1} in Al_2O_3) (Ref. 15) showing that the OsO_6 framework remains very rigid over the temperature range of 2–350 K. The slower thermal expansions of the potassium and rubidium materials compared to $CsOs_2O_6$ are noteworthy and are, in part, derived from the very marked non-Grüneisen behavior for KOs_2O_6 and similar, though less marked, behavior for $RbOs_2O_6$ again below ~80 K. With KOs_2O_6, the lattice parameter is almost invariant and/or slightly decreases on heating from 1.5 to 12 K followed by a relatively rapid increase between 15 and ~80 K and a much less steep increase from 80 to 180 K with an increasingly rapid expansion on further heating to 500 K. Such behavior and the very low overall thermal expansion coefficient derived are indicative of more complex structural behavior than simple increases in effective bond lengths caused by thermal motion.

Further analysis of the diffraction data from KOs_2O_6 therefore centered on possible origins of this effect and also investigation of the models developed by Schuck *et al.*[5] from single crystal x-ray diffraction data in the temperature range of 80–400 K. Furthermore, the 1.5 K data set was analyzed in detail with the aim of finding evidence for the structural transition at 7 K proposed by Hiroi *et al.*[8] Initially, the profiles were examined for the evidence of additional reflections which would support the lower $F\text{-}43m$ symmetry proposed by Schuck *et al.*[5] Figure 2 shows the experimental profiles between 67° and 69° for the 1.5 K data and the summed, every 25 K (to improve statistics), data sets between 10 and 475 K. The inset shows the calculated profile in this region based on the model and coordinates previously proposed;[5] all data, experimental and theoretical, have been scaled so that the adjacent reflection at $2\theta=67°$, $(hkl)=(531)$, is of identical intensity. As can be seen from these profiles, there is no evidence of a concerted phase change or lowering of symmetry from $Fd\text{-}3m$ to $F4\text{-}3m$. Indeed, Le Bail extractions, varying just profile parameters, carried out on data sets collected at between 1.5 and 475 K in $Fd\text{-}3m$ and $F4\text{-}3m$ showed no significant variation in the extracted profile fit factors confirming that the space group needed to describe the structure across this whole temperature range remains

TABLE I. 1.5 K structure model 1 for KOs_2O_6 and extracted key distances and angles. $a=10.0889(1)$ Å, $Fd\text{-}3m$, $wR_p=0.0426$, and $R_p=0.0303$. K-O×12 [3.0915(9 Å)], Os-O×6 [1.9092(3) Å], and OS-O-Os [137.81(5)°].

Name/site	x	y	z	$U_i/U_e\times100/\text{Å}^2$	Site occupancy
K 8*b*	0.375	0.375	0.375	2.95(11)	1.0
Os 16*d*	0.0	0.0	0.0	1.16(3)	1.0
O 48*f*	0.31820(9)	0.125	0.125	1.40(4)	1.0

TABLE II. 1.5 K structural model 2 for KOs_2O_6 and extracted key distances and angles. a =10.0889(1) Å, *Fd*-3*m*, wR_p=0.0413, and R_p=0.0288. K-O×6 [2.941(18)×3. 3.26(22)×3, and 3.361(31)×3 Å], Os-O×6 [1.9089(3) Å], and Os-O-Os [137.86(5)°].

Name/site	x	y	z	$U_i/U_e\times 100/\text{Å}^2$	Site occupancy
K 32*e*	0.3591(20)	0.3591(20)	0.3591(20)	0.21(13)	0.25
Os 16*d*	0.0	0.0	0.0	1.14(25)	1.00
O1 48*f*	0.31811(9)	0.125	0.125	1.38(4)	1.0000

unchanged. No difference in the extracted Le Bail profile fit parameters between *F*4-3*m* and *Fd*-3*m* was observed at any temperature either.

Therefore, all further modeling was undertaken in *Fd*-3*m*, but various models within this space group were investigated. At the higher temperatures of 100–500 K, with high thermal motion of the species present, the profiles were best fitted using the standard *Fd*-3*m* pyrochlore description (denoted as model 1) with a high atomic displacement parameter for potassium which represents very well the thermal motion of the potassium ion within the large cavity surrounding 8*b* (Table I). At low temperatures, the best model (model 2) involved a static disordered displacement of the potassium ion from 8*b* to 32*e* with a site occupancy of $\frac{1}{4}$. In this model, Table II summarizes the coordinate description showing a significant displacement of the potassium ion from the central position (magnitude of ~0.23 Å, Fig. 3); On this site, this also results in a much lower atomic displacement parameter for the ion. Comparison of the profile fits achieved with models 1 and 2 to the 1.5 K data set showed a small improvement in the profile fit factors (Tables I and II)—it should be noted that these two models are effectively similar representation of the scattering density of KOs_2O_6 at low temperature. The stable refinement of a significant displacement of the potassium ion and reduced (far more realistic) atomic displacement parameter for potassium supports model 2 as a better representation of KOs_2O_6 at low temperature. Figure 4 shows the final, excellent fit achieved to the diffraction data profile. As a final check on the possibility of the *F*-43*m* model,[4,5] additional refinements were carried out in this space group using an ordered potassium ion distribution and then allowing one potassium ion which showed a large atomic displacement parameter when on a special site to become displaced. For both refinements simultaneously varying the positional and atomic displacement parameters produced an unstable refinement, so these were varied only in alternate cycles. Tables III and IV summarize the results of these analyses. For the model of Schuck *et al.*[5] (Table III), the quality of the fit to the data was similar to that obtained with the ordered *Fd*-3*m* description (Table I) and with an elevated atomic displacement parameter for the potassium ion on the 4*c* site. However the increased number of refinable parameters and instability in the refinement does not support this model over model 1. Disordering of the potassium from 4*c* to 16*e* resulted in a more reasonable ADP for this ion but no improvement in profile fit. Overall the absence of reflections requiring a reduction in symmetry to *F*-43*m* and the inability to improve the profile fit by modeling in this space group supports model 2 as the best description of the KOs_2O_6 structure at low temperature.

In order to investigate any change in the suitability of these models as a function of temperature, a SEQGSAS[13] re-

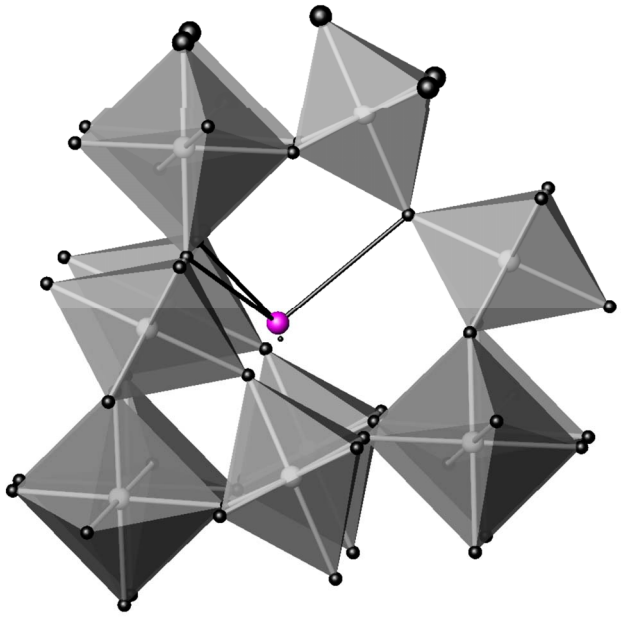

FIG. 3. (Color online) Structure model demonstrating the displacement of the potassium ion (shaded sphere with coordination to oxygen shown) from the central 8*b* site (●). Shaded polyhedra are OsO_6.

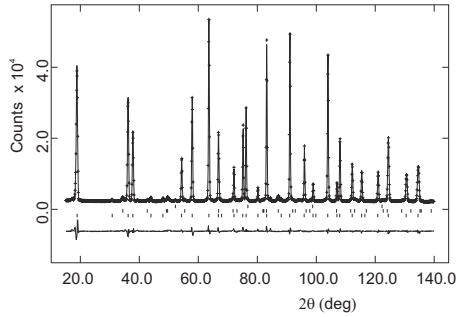

FIG. 4. Profile fit obtained to the 1.5 K data set obtained from KOs_2O_6 (1200 s data set). Cross marks are observed intensities, upper continuous line is the calculated profile, and lower continuous line is the difference. Tick marks, from top to bottom, are calculated reflection positions for KOs_2O_6, OsO_2, and vanadium (sample can).

TABLE III. 1.5 K structure model 3 for KOs_2O_6. $a=10.0889(1)$ Å, F-43m, ordered potassium ions $wR_p=0.0429$, and $R_p=0.0304$.

Name/site	x	y	z	$U_i/U_e\times 100/\text{Å}^2$	Site occupancy
K 4c	0.25	0.25	0.25	5.32	1.0
K 8b	0.5	0.5	0.5	1.08	1.0
Os 16e	0.8766(3)	0.8766(3)	0.8766(3)	1.20	1.0
O 24f	0.1920(6)	0.0	0.0	1.85	1.0
O 24g	0.5554(5)	0.25	0.25	0.98	1.0

finement of the structure using the individual data sets from 1.5 to 275 K was undertaken using model 2 as the starting point. Figure 5 shows the extracted potassium ion displacement from the 8b position and Fig. 6 this ion's ADP as a function of temperature. As the temperature is raised, the magnitude of this static displacement shows a tendency to decrease with an increasing e.s.d. while the extracted atomic displacement parameter markedly increases so that structural description effectively becomes indistinguishable from model 1 above about 80 K. Indeed, for data sets collected above 80 K, model 1 could be used to fit the profiles generating identical fit factors to model 1 with of course fewer refinable parameters. It is noteworthy that this change in preferred model occurs in the same temperature range where the plateau is reached in the lattice parameter variation. This implies that the confinement of the potassium ion to one side of the cavity may occur on cooling below approximately 80 K and result in a marked more rapid decrease in lattice parameter. The process seems to be complete by around 10–20 K where the lattice parameter [Fig. 1(a), inset] levels out and then slightly expands on cooling further to 1.5 K.

For $RbOs_2O_6$, similar behavior is observed though the deviations in the lattice parameter variation are not as strong as with the potassium analog. The lattice parameter is again almost invariant below 10 K before an initial relatively rapid increase between 10 and 50 K; a weak plateau exists between 50 and 100 K before more normal expansion at higher temperatures. As noted in our previous work on this material, the structure can be successfully modeled in the Fd-3m description between 2 and 450 K though with a somewhat high compared to those of osmium and oxygen atomic displacement parameter for rubidium. Following the observation of a refinable off-center displacement for potassium in KOs_2O_6, we investigated whether a similar displacement could be determined for rubidium in $RbOs_2O_6$ using the data collected here at 1.5 K and in our previous D2B experiment on this compound.[12] Structure refinements displacing Rb to the 32e site (x,x,x) produced only a very marginal improvement in profile fit a slight reduction in this atom's ADP, and a value of 0.368(5) for x showing that the displacement of this species probably occurs but is not crystallography significant that is cit is less than two e.s.d. from the central site at $x=0.375$. However, it seems likely that the variations in lattice parameter in $RbOs_2O_6$ below 50 K result from a similar behavior to that observed with KOs_2O_6, and localized static displacements of the rubidium ions to the 32e sites occur on cooling between 25 and 10 K. It is noteworthy that the temperature at which the static displacements of the A-type cation start to occur (and are reflected in a more rapid decrease in the lattice parameter) is lower for Rb (below around 50 K) than for K (below around 80 K).

B. $ANbTeO_6$, A=K Rb, and Cs

As with the beta-pyrochlore osmates, initial analysis of the diffraction data centered on extracting the lattice parameter as a function of temperature (Fig. 7). Data from the A=Rb and Cs systems showed typical Grüneisen-type behaviors, but for A=K, anomalous variation was found below 70 K. This can also be observed in the average thermal expansion coefficients between 10 and 500 K which are 4.20×10^{-6} K^{-1} (Cs) 4.06×10^{-6} K^{-1} (Rb), and 3.15×10^{-6} K^{-1} (K). For $KNbTeO_6$, the lattice parameter is almost invariant on cooling from 70 to 40 K, which rapidly contracts between 35 and 15 K before leveling off or possibly showing slight expansion on cooling below 10 K. This behavior is very similar to that observed with KOs_2O_6 and implies freezing out of a potassium ion displacement at these low tem-

TABLE IV. 1.5 K structure model 3 for KOs_2O_6. $a=10.0889(1)$ Å, F-43m, one disordered potassium ion $wR_p=0.0432$, and $R_p=0.0307$.

Name/site	x	y	z	$U_i/U_e\times 100/\text{Å}^2$	Site occupancy
K 16e	0.2678(7)	0.2678(7)	0.2678(7)	3.12	0.25
K 8b	0.5	0.5	0.5	0.60	1.0
Os 16e	0.8768(3)	0.8768(3)	0.8768(3)	1.21	1.0
O 24f	0.1929(6)	0.0	0.0	1.62	1.0
O 24g	0.5561(5)	0.25	0.25	1.26	1.0

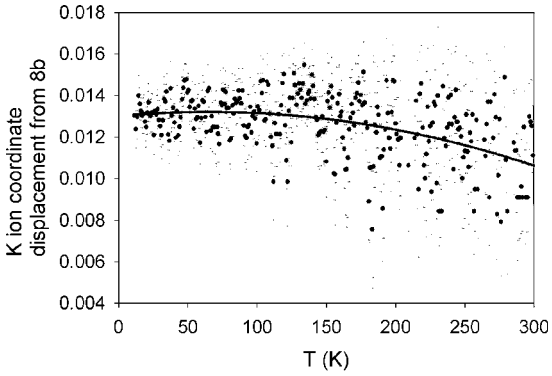

FIG. 5. The refined coordinate displacement of K^+ from the 8*b* site in model 2 as a function of temperature.

peratures. Detailed analysis of the 2 K data set showed that the potassium ion is displaced onto (x,x,x) with $x=0.355(2)$. The larger displacement ~0.35 Å, (cf. 0.23 Å for potassium in KOs_2O_6) for the potassium ion in $KNbTeO_6$ probably reflects the larger lattice parameter and hence larger volume cavity occupied by the potassium ion.

IV. DISCUSSION

The behaviors of the structures of the AOs_2O_6 phases as a function of temperature reflect the ionic sizes of the *A* ions. For *A*=Cs, the behavior is classical between 2 and 350 K with a variation in lattice parameter that can be well fitted using simple Grüneisen theory though with a small overall thermal expansion parameter, indicative of a rigid osmium-oxygen framework. For *A*=K, the lattice parameter behavior as a function of temperature is much more complex indicating some structural changes on cooling from room temperature. Analysis of these data indicates that at low temperatures between 80 and 20 K, the rattling of the potassium ion is gradually frozen out with the ion strongly coordinating to one side of the cavity; hopping of potassium ions between the off-center sites is likely to occur in this temperature range and may still slowly occur below 20 K though dynamic measurements such as inelastic neutron scattering would be required to investigate this behavior.

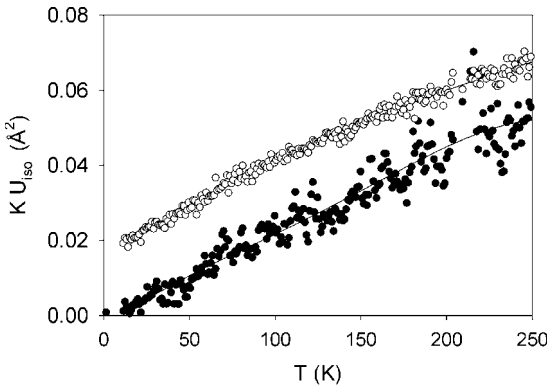

FIG. 6. U_i as a function of temperatures for potassium in model 1 (○) and model 2 (●).

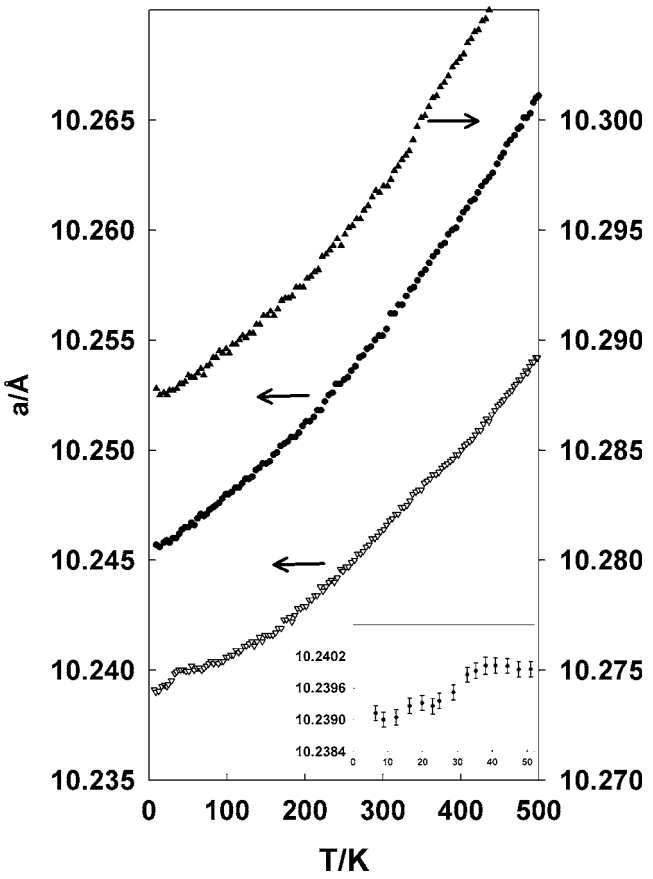

FIG. 7. Lattice parameters of all $ANbTeO_6$ phases as a function of temperature. Inset: $KNbTeO_6$, *K*=▽, Rb=●, Cs=▲.

In this analysis of polycrystalline material, this trapping of the cation seems to randomly occur leaving the *Fd*-3*m* description with statically disordered potassium ions as the best model. It is possible that in single crystals, such displacements of the potassium ions could occur in a more concerted manner in portions of the crystal leading to domains of lower symmetry. If such domains were large enough, then single crystal diffraction studies might show extra reflections consistent with the lower symmetry of the ordered regions. Here, no further structural changes could be determined for KOs_2O_6 samples cooled below 7 K indicating that any structural effects associated with the first order phase transition believed to occur[9] are very minor. However the very weak negative thermal expansion that occurs on cooling below ~10 K may be associated with further very small and local static displacements of the potassium ions to for example even lower symmetry sites such as 96 g (x,x,z). It is possible that any such further very small local displacements of potassium ions could be tied to the superconducting transition or the phase transition at 7 K, but a probe of the potassium ion's local symmetry such as extended x-ray-absorption fire structure or NMR would be needed to resolve this. The structural changes that occur in $RbOs_2O_6$ as a function of temperature are intermediate between those of the potassium and cesium analogs with a weaker but observable effect involving rubidium ion displacements below ~50 K. The behavior of $KNbTeO_6$ mirrors that of KOs_2O_6 though the lo-

calization of the potassium ions is even more strongly defined in terms of the size of potassium ion displacement and the differential rates of thermal expansion seen in the lattice parameter temperature variation.

Very similar structural behaviors have been observed in other materials where delocalization or detrapping of an atom from split and partially occupied sites occurs as a function of temperature. In Ba_6Ge_{25}, the structure at low temperature is modeled with the barium atom split over two sites whose separation markedly varies as a function of temperature while at around room temperature, a fully ordered model can be used. The transition between these models occurs between 250 and 200 K and is associated with negative thermal expansion of the material; these structural effects in this material are associated with a marked drop in the electrical conductivity.[16]

V. CONCLUSIONS

At very low temperatures, the structures of the beta-pyrochlores AB_2O_6 for the smaller cations A are best described in terms of disordered localized A-type cations. For KOs_2O_6, a local displacement of the potassium ion starts to become apparent below ~80 K and is complete above T_C. Thus, any discussion of the structure and derived properties of the superconducting pyrochlore osmate phases should employ a structural model with locally displaced alkali metal cations. At high temperatures above ~80 K a model with full rattling of the A-type cations around a central pyrochlore cavity position best describes the structure.

ACKNOWLEDGMENTS

The authors acknowledge EPSRC for support for this work under Grant No. EP/D00386 and the ILL for the provision of neutron beamtime (Expt. No. 5-24-270). We also thank C. S. Knee University of Gothenburg, for useful discussions.

[1] S. Yonezawa, Y. Muraoka, and Z. Hiroi, J. Phys. Soc. Jpn. **73**, 1655 (2004).
[2] S. Yonezawa, Y. Muraoka, Y. Matsushita, and Z. Hiroi, J. Phys. Soc. Jpn. **73**, 819 (2004).
[3] S. Yonezawa, Y. Muraoka, Y. Matsushita, and Z. Hiroi, J. Phys.: Condens. Matter **16**, L9 (2004).
[4] G. Schuck, S. M. Kazakov, K. Rogacki, N. D. Zhigadlo, and J. Karpinski, Phys. Rev. B **73**, 144506 (2006).
[5] G. Schuck, J. Karpinski, Z. Bukowski, and D. Chernyshov, *Temperature Dependent Structural Studies of Beta-pyrochlore* KOs_2O_6 *Single Crystals* (Jahrestagung der Deutsche Gesellschaft für Kristallographie, Bremen, Germany, 2006).
[6] J. I. Yamaura, S. Yonezawa, Y. Muraoka, and Z. Hiroi, J. Solid State Chem. **179**, 336 (2006).
[7] J. Kuneš, T. Jeong, and W. E. Pickett, Phys. Rev. B **70**, 174510 (2004).
[8] Z. Hiroi, S. Yonezawa, and J. Yamaura, J. Phys.: Condens. Matter **19**, 145283 (2007).
[9] K. Sasai, K. Hirota, Y. Nagao, S. Yonezawa, and Z. Hiroi, J. Phys. Soc. Jpn. **76**, 104603 (2007).
[10] Z. Hiroi, S. Yonezawa, Y. Nagao, and J. Yamaura, Phys. Rev. B **76**, 014523 (2007).
[11] R. Galati, C. Simon, C. S. Knee, P. F. Henry, B. D. Rainford, and M. T. Weller, Chem. Mater. **20**, 1652 (2008).
[12] R. Galati, R. W. Hughes, C. S. Knee, P. F. Henry, and M. T. Weller, J. Mater. Chem. **17**, 160 (2007).
[13] A. C. Larson and R. B. Von Dreele, Report No. MS-H805, 1990 (unpublished).
[14] B. H. Toby, J. Appl. Crystallogr. **34**, 210 (2001).
[15] F. S. Galasso, *Perovskites and High Tc Superconductors* (Gordon and Breach Science, New York, 1990).
[16] M. Schmidt, P. G. Radaelli, M. J. Gutmann, S. J. L. Billinge, N. Hur, and S. W. Cheong, J. Phys.: Condens. Matter **16**, 7287 (2004).